JPET Fast Forward. Published on October 28, 2014 as DOI: 10.1124/jpet.114.218644
This article has not been copyedited and formatted. The final version may differ from this version.

The Antiparasitic Drug, Potassium Antimony Tartrate, Inhibits Tumor Angiogenesis and Tumor Growth in Non-Small Cell Lung Cancer

Beibei Wang, Weiwei Yu, Jiawei Guo, Xingwu Jiang, Weiqiang Lu, Mingyao Liu, Xiufeng Pang

Shanghai Key Laboratory of Regulatory Biology, Institute of Biomedical Sciences and School of Life Sciences, East China Normal University, Shanghai, China (*B.W., W.Y., J.G., X.J., W.L., M.L., X.P.*); Institute of Biosciences and Technology, Department of Molecular and Cellular Medicine, Texas A&M University Health Science Center, Houston, Texas, USA (*M.L.*)

Downloaded from jpet.aspetjournals.org at ASPET Journals on April 17, 2024

JPET Fast Forward. Published on October 28, 2014 as DOI: 10.1124/jpet.114.218644
This article has not been copyedited and formatted. The final version may differ from this version.

Running title: Potassium antimony tartrate inhibits angiogenesis

To whom correspondence should be addressed:

Drs. Xiufeng Pang or Mingyao Liu, Shanghai Key Laboratory of Regulatory Biology, The Institute of Biomedical Sciences and School of Life Sciences, East China Normal University, 500 Dongchuan Road, Shanghai 200241, China. Phone: +86-21-24206942; Fax: +86-21-54344922; E-mail: xfpang@bio.ecnu.edu.cn; myliu@bio.ecnu.edu.cn

Number of text pages: 43

Number of tables: 1

Number of figures: 6

Number of references: 48

Number of words in Abstract: 246

Number of words in Introduction: 714

Number of words in Discussion: 1123

List of nonstandard abbreviations:

NSCLC	non-small cell lung cancer cells
HUVECs	human umbilical vein endothelial cells
PAT	potassium antimonyl tartrate
VEGF	vascular endothelial cell growth factor
FGF	fibroblast growth factor
RTKs	receptor tyrosine kinases

Downloaded from jpet.aspetjournals.org at ASPET Journals on April 17, 2024

JPET Fast Forward. Published on October 28, 2014 as DOI: 10.1124/jpet.114.218644
This article has not been copyedited and formatted. The final version may differ from this version.

FAK	focal adhesion kinase
ERK	extracellular signal-regulated kinase
RTKIs	receptor tyrosine kinase inhibitors
EGM-2	endothelial cell growth medium-2

Recommended section assignment: Drug Discovery and Translational Medicine

Downloaded from jpet.aspetjournals.org at ASPET Journals on April 17, 2024

JPET Fast Forward. Published on October 28, 2014 as DOI: 10.1124/jpet.114.218644
This article has not been copyedited and formatted. The final version may differ from this version.

Abstract

Repurposing existing drugs not only accelerates drug discovery but rapidly advances clinical therapeutic strategies. In this article, we identified potassium antimonyl tartrate (PAT), an antiparasitic drug, as a novel agent to block angiogenesis by screening Food and Drug Administration-approved chemical drugs. By comparing the cytotoxicity of PAT in various non-small cell lung cancer cells (NSCLC) with that observed in primary cultured human umbilical vein endothelial cells (HUVECs), we found that HUVECs were much more sensitive to the PAT treatment. In *in vivo* tumor xenograft mouse models established either by PAT-resistant A549 cells or by patient primary tumors, PAT significantly decreased the tumor volume and tumor weight of NSCLC xenografts at dose of 40 mg/kg (i.p., daily) and, more importantly, augmented the antitumor efficacy of cisplatin chemotherapy. Remarkable loss of vascularization in the treated xenografts indicated the *in vivo* anti-angiogenesis property of PAT, which was well-correlated with its tumor growth inhibition in NSCLC. Furthermore, in the *in vitro* angiogenic assays, PAT exhibited dose-dependent inhibition of HUVEC proliferation, migration and tube formation in response to different stimuli. Consistently, PAT also abolished the vascular endothelial cell growth factor (VEGF)-induced angiogenesis in the Matrigel plugs assay. Mechanistically, we found that PAT inhibited the activities of several receptor tyrosine kinases and specifically blocked the activation of downstream Src and focal adhesion kinases in HUVECs. Taken together, our results characterized the novel antiangiogenic and antitumor function of PAT in NSCLC. Further study of PAT in

Downloaded from jpet.aspetjournals.org at ASPET Journals on April 17, 2024

JPET Fast Forward. Published on October 28, 2014 as DOI: 10.1124/jpet.114.218644
This article has not been copyedited and formatted. The final version may differ from this version.

anticancer clinical trials may be warranted.

Downloaded from jpet.aspetjournals.org at ASPET Journals on April 17, 2024

JPET Fast Forward. Published on October 28, 2014 as DOI: 10.1124/jpet.114.218644
This article has not been copyedited and formatted. The final version may differ from this version.

Introduction

Angiogenesis, the generation of new blood vessels from the pre-existing vasculature, is responsible for the metabolic demands of all types of solid tumors (Hanahan and Folkman, 1996). Tumors secrete several proangiogenic factors stimulating endothelial cell migration, proliferation and capillary-like tube formation, thus satisfying the requirement for tumor growth and metastasis (Asahara et al., 1995; Niki et al., 2000). Inhibition of growth factor signals requisite for endothelial cells has become a therapeutic strategy (Algire et al., 1954; Folkman, 1971). In fact, no identical pattern of angiogenesis has been found in tumors, indicating that angiogenesis is comprehensively triggered and mediated by different pathways (Lund et al., 1998). Several regulatory and signaling molecules controlling angiogenesis have been characterized, including potent growth factors [e.g., vascular endothelial growth factor (VEGF), fibroblast growth factor (FGF) and angiopoietin] (Ferrara and Kerbel, 2005; Presta et al., 2005; Saharinen et al., 2011), receptor tyrosine kinases (RTKs) (Jeltsch et al., 2013), and molecules involved in signaling cascades, such as Src kinase, focal adhesion kinase (FAK), extracellular signal-regulated kinase (ERK), and AKT (Downward, 2003; McLean et al., 2005; Kim et al., 2009; Liu et al., 2009; Lemmon and Schlessinger, 2010). These molecules have been exploited for their potential as drug targets for anti-angiogenic therapy. It is generally agreed that multiple signaling pathways should be coordinately blocked in the treatment of solid tumors to achieve maximal angiogenesis inhibition.

Downloaded from jpet.aspetjournals.org at ASPET Journals on April 17, 2024

JPET Fast Forward. Published on October 28, 2014 as DOI: 10.1124/jpet.114.218644
This article has not been copyedited and formatted. The final version may differ from this version.

Lung cancer, a type of heterogeneous solid tumors, is the leading cause of cancer-related deaths in both sexes worldwide (Siegel et al., 2013). Non-small cell lung cancer (NSCLC), which accounts for approximately 85% of all lung cancer cases, possesses several critical hallmarks, such as sustained angiogenesis, addiction to aerobic glycolysis and self-sufficiency in growth signals (Siegel et al., 2012). In 2006, the US Food and Drug Administration (FDA) approved bevacizumab, a VEGF-A monoclonal antibody, as the first anti-angiogenic agent for treatment of patients suffering from NSCLC (Ferrara et al., 2004; Sandler et al., 2006). However, toxicities, substantial cost and modest survival rates successively occurred (Ranpura et al., 2011). Recently, small molecule receptor tyrosine kinase inhibitors (RTKIs) and monoclonal antibodies targeting endothelial cells have shown promise in NSCLC treatment when combined with standard chemotherapy, but their efficacy remains to be decided (Sennino and McDonald, 2012). A second phase III trial of sorafenib, a multi-targeted antiangiogenic RTKI, combined with gemcitabine/cisplatin in a first-line setting in NSCLC patients has shown an improvement in progression-free survival rate but not in overall survival rate (Paz-Ares et al., 2012). More affordable and effective antiangiogenic agents are still greatly desirable.

Over the past decade, an effective approach to accelerate drug development has been proposed and gained considerable attention (Chong and Sullivan, 2007). This approach is termed “drug repurposing”, “drug repositioning”, “drug re-profiling” or “indication switching”. Due to established drugs possessing well-known safety and pharmacokinetic profiles, identification of new applications of approved drugs could

Downloaded from jpet.aspetjournals.org at ASPET Journals on April 17, 2024

JPET Fast Forward. Published on October 28, 2014 as DOI: 10.1124/jpet.114.218644
This article has not been copyedited and formatted. The final version may differ from this version.

be rapidly evaluated in Phase II and III clinical studies. Recently, many existing non-cancer drugs have entered into clinical trials for cancer-related treatment, such as thalidomide (D'Amato et al., 1994), nonsteroidal agents (Jones et al., 1999) and rapamycin (Guba et al., 2002), in which promising clinical results have been achieved. Following the hypothesis of drug indication switching, we performed the screening of existing drugs against tumor angiogenesis using a panel of NSCLC cells and primary cultured human umbilical vein endothelial cells (HUVECs). We found that the cytotoxicity of potassium antimonyl tartrate (PAT), a long-term use antiparasitic, specifically targeted HUVECs, rather than NSCLC cells, suggesting its potential antiangiogenic activity.

PAT is a trivalent antimonial salt that has previously been applied as an antiparasitic agent in the treatment of leishmaniasis and schistosomiasis for more than 100 years. PAT interferes with phosphofructokinase and the thiol redox potential of the parasite (Schulert et al., 1966). Initially reported by Lecureur and colleagues, PAT, which is similar to As_2O_3, was found to be cytotoxic towards acute promyelocytic leukemia (Lecureur et al., 2002a; Lecureur et al., 2002b). However, a more complete characterization of its anticancer role is still limited, especially in solid tumors. In this article, we evaluated the putative antiangiogenic activities of PAT in a series of *in vitro* and *in vivo* tumor preclinical models. Our data revealed that PAT notably retards tumor growth and potentiates the efficacy of standard chemotherapy in human NSCLC by blocking tumor angiogenesis.

Downloaded from jpet.aspetjournals.org at ASPET Journals on April 17, 2024

JPET Fast Forward. Published on October 28, 2014 as DOI: 10.1124/jpet.114.218644
This article has not been copyedited and formatted. The final version may differ from this version.

Materials and Methods

Reagents

PAT (purity > 99%) was obtained from Sigma (St. Louis, MO), and PAT stock solutions were prepared with dimethyl sulfoxide (DMSO; Sigma) for *in vitro* assays. For *in vivo* experiments, PAT and cisplatin (Sigma) were diluted in phosphate buffered saline (PBS). Recombinant human $VEGF_{165}$ and $bFGF_{146}$ were gifted from the Experimental Branch of the NIH (Bethesda, MD), and Angiogenin-1 (Ang-1) was purchased from RayBiotech (Norcross, GA). Growth factor–reduced Matrigel was purchased from BD Biosciences (San Jose, CA), and calcein-AM was obtained from Sigma. The human RTK phosphorylation antibody array was purchased from RayBiotech. For Western blotting analysis, anti-VEGFR2, anti-$pTyr^{1175}$-VEGFR2, anti-$pTyr^{996}$-VEGFR2, anti-Tie2, anti-$pTyr^{416}$-Src, anti-Src, anti-$pTyr^{397}$-FAK, anti-FAK, anti-$pThr^{202}$/Tyr^{204}-ERK, anti-ERK1/2, anti-$pSer^{473}$-AKT, anti-AKT, and anti-β-actin antibodies were purchased from Cell Signaling Technology (Beverly, MA). For the immunofluorescence and immunohistochemistry analyses, the antibody against CD31 was purchased from Abnova (Taipei, Taiwan), and the Ki-67 antibody was purchased from Cell Signaling Technology. The non-radioactive cell proliferation kit was purchased from Promega (Madison, WI). All other chemicals used in this study were ACS reagents.

Cell lines and cell culture

Primary human umbilical vascular endothelial cells (HUVECs) were kindly provided

Downloaded from jpet.aspetjournals.org at ASPET Journals on April 17, 2024

JPET Fast Forward. Published on October 28, 2014 as DOI: 10.1124/jpet.114.218644
This article has not been copyedited and formatted. The final version may differ from this version.

by Dr. Xinli Wang (Baylor College of Medicine, Houston, TX) in 2008 and cultured in endothelial cell growth medium-2 (EGM-2; Lonza, Basel, Switzerland) according to the manufacturer's instructions. Angiogenesis stimulation medium was defined as EGM-2 basal media containing 0.5% fetal bovine serum (FBS; HyClone Laboratories, Logan, UT) and supplemented with the following growth factors: VEGF (50 ng/mL), bFGF (12 or 50 ng/mL) or Ang-1 (200 ng/mL). NSCLC cell lines (A549, PC9, NCI-H460, NCI-H441, NCI-H522 and NCI-H661) were obtained from the American Type Culture Collection (Manassas, VA) in 2010 and cultured in RPMI 1640 medium containing 10% FBS. Human fetal lung fibroblast cells (WI-38) and human pulmonary fibroblast cells (MRC-5) were obtained from the National Platform of Experimental Cell Resource for Sci-Tech (Shanghai, China) in 2012 and cultured in Eagle's Minimal Essential Media containing 10% FBS and 1% penicillin/streptomycin, kanamycin sulfate and glutamax. All cell lines have been tested and authenticated by DNA (short tandem repeat genotyping) profiling. The last test was performed in March 2013. All of these cells were grown at 37°C under a humidified 95:5 (%; v/v) mixture of air and CO_2.

Cell proliferation assays

HUVECs (2-5×10^3 cells/well) were first starved and then treated with various concentrations of PAT in either EGM-2 or angiogenesis stimulation medium for 72 h. A549, PC9, NCI-H460, NCI-H441, NCI-H522, NCI-H661, WI-38 and MRC-5 cells (4-6×10^3 cells/per well) were directly exposed to indicated concentrations of PAT in full growth medium for 72 h. To determine cell viability, we used a non-radioactive

Downloaded from jpet.aspetjournals.org at ASPET Journals on April 17, 2024

JPET Fast Forward. Published on October 28, 2014 as DOI: 10.1124/jpet.114.218644
This article has not been copyedited and formatted. The final version may differ from this version.

cell proliferation kit containing a tetrazolium compound [3-(4,5-dimethylthiazol-2-yl)-5-(3-carboxymethoxyphenyl)-2-(4-sulfophenyl)-2H-tetrazolium, inner salt; MTS] and a VERSAmax microplate reader (Molecular Devices; Sunnyvale, CA). The half inhibitory concentration (IC_{50}) values were calculated by Graphpad Prism software (GraphPad Software, La Jolla, CA). Each assay was performed at least three times and each treatment had four repeats.

Animal studies

BALB/cA nude mice, immunodeficient NOD/SCID mice and C57BL/6 mice used in the present study were purchased from National Rodent Laboratory Animal Resources (Shanghai, China) and maintained in a laminar airflow cabinet under specific pathogen-free conditions and a 12 h light–dark cycle. All treatments were administered according to the NIH standards established in the Guidelines for the Care and Use of Experimental Animals, and all the protocols were approved by East China Normal University.

Human NSCLC tumor xenograft mouse model

Cultured NSCLC cell xenograft mouse model. The cultured NSCLC cell xenograft mouse model was constructed as described previously (Pang et al., 2009b). A549 cells (5×10^6 cells/mouse) were injected s.c. into the right flank of 5- to 6-week-old male BALB/cA nude mice. Tumor size was evaluated every other day by caliper measurements, and the approximate volume of the tumor mass was calculated using the following formula: $V = (L + [W]^2) \times 0.52$; where L is the longest diameter of the

Downloaded from jpet.aspetjournals.org at ASPET Journals on April 17, 2024

JPET Fast Forward. Published on October 28, 2014 as DOI: 10.1124/jpet.114.218644
This article has not been copyedited and formatted. The final version may differ from this version.

tumor; and W is the shortest diameter of the tumor. Tumor-bearing mice with an average tumor volume exceeding approximately 150 mm^3 were randomly divided into the following groups: vehicle control (PBS; i.p.; daily); PAT (40 mg/kg; i.p.; daily); cisplatin (4 mg/kg; i.p.; weekly); or a combination of PAT and cisplatin (n=8 each group). All groups were continuously administered for 34 d, and the body weight was measured every other day. At the end of the experiment, mice were sacrificed. Solid tumors were removed, weighed and processed for immunofluorescence and immunohistochemistry.

Primary NSCLC tumor xenograft mouse model. The primary mouse model was established as previously described (Migliardi et al., 2012). Surgical samples of patient primary NSCLC presenting adenocarcinoma histology were obtained from treatment-naïve patients at the Shanghai Changzheng Hospital (Shanghai, China). Prior written informed consent was obtained from all patients, and the study protocol was approved by the local hospital ethics committee. In brief, surgically removed tumor tissues were cut into fragments of approximately 15 mm^3 and implanted using a trocar needle s.c. into 2-3 male NOD/SCID mice within 2 h. Transplanted mice bearing xenografts were observed weekly. When tumor volume reached approximately 1000 mm^3, primary xenografts at the exponential growth phase were removed by serially passage to other immunodeficient mice. After three consecutive mouse-to-mouse passages, the xenograft was considered to be stabilized and submitted to mutation analyses to verify that it consistently maintained clinical NSCLC molecular features. “Hot spot” mutations in *EGFR* (exons 18, 19 and 21),

Downloaded from jpet.aspetjournals.org at ASPET Journals on April 17, 2024

JPET Fast Forward. Published on October 28, 2014 as DOI: 10.1124/jpet.114.218644
This article has not been copyedited and formatted. The final version may differ from this version.

KRAS (exons 2 and 3), *PIK3CA* (exons 9 and 20), and *BRAF* (exon 15) were screened by direct sequencing. Numerous samples from early passages were immediately stored in liquid nitrogen and used for further experiments. Xenografts at passage 3 were used in this study. Mice were treated using the same conditions as in the cultured NSCLC cell xenograft mouse model. On day 28, the solid tumors were harvested, weighed and analyzed for indicated protein markers.

Immunofluorescence and immunohistochemistry

As described previously (Qian et al., 2013), the solid tumors were fixed, dehydrated, and embedded in paraffin. Serial sections (4 μm thick) were cut, mounted on adhesion microscope slides, dewaxed in xylene and rehydrated in gradient alcohols. After quenching the endogenous peroxidase activity and antigen retrieval, the sections were blocked with 1% bovine serum albumin and incubated with primary antibody overnight. For tissue localization of Ki-67 and CD31, sections were incubated with secondary antibody at room temperature (20 min for immunohistochemistry and 1 h for immunofluorescence). Sections were then visualized by the streptavidin-biotin-peroxidase complex method with 3,3'-diaminobenzidine and counterstained with hematoxylin (immunohistochemistry) or DAPI (immunofluorescence) as the chromogen. Each group had at least six samples, and sections from the same tumor were processed in parallel from at least three samples. Images were taken using a leica DM4000B photo microscope (magnification of 200×).

Downloaded from jpet.aspetjournals.org at ASPET Journals on April 17, 2024

JPET Fast Forward. Published on October 28, 2014 as DOI: 10.1124/jpet.114.218644
This article has not been copyedited and formatted. The final version may differ from this version.

Cell migration assays

Endothelial cell migration assay. HUVECs were allowed to grow to full confluence in 6-well plates precoated with 0.1% gelatin (Sigma). To inactivate cell proliferation, HUVECs were first synchronized with EGM-2 basal medium containing 0.5% FBS for 6 h. The cells were then wounded with pipette tips and washed with PBS followed by exposure to EGM-2 medium containing PAT (0-10 μmol/L) or DMSO. Following 8-10 h of migration, cells were labeled with 2 mg/mL calcein-AM for 30 min and visualized using an inverted microscope (Olympus; magnification of 64×). Migrated cells in four random fields were quantified by manual counting. Three independent experiments in triplicate were performed.

Endothelial cell Transwell migration assay. The chemotactic motility of HUVECs was determined using a Transwell migration assay (BD Biosciences; San Jose, CA) with 6.5-mm diameter polycarbonate filters (8-mm pore size) as described previously (Pang et al., 2009a). Briefly, the filter was coated with gelatin. Angiogenesis stimulation medium (500 μL) was placed into the bottom chambers. HUVECs ($4\text{-}5\times10^4$) were incubated with indicated concentrations of PAT in EGM-2 containing 0.5% FBS for 30 min at 37°C before seeding into the upper chambers. After 8-10 h of incubation, non-migrated cells in the upper chamber were removed using a cotton swab. The migrated cells were fixed with 4% paraformaldehyde and stained with 1% crystal violet. Images were taken using an Olympus inverted microscope (magnification of 160×). Migrated cells in four random fields were quantified by manual counting. Three independent experiments were performed.

Downloaded from jpet.aspetjournals.org at ASPET Journals on April 17, 2024

JPET Fast Forward. Published on October 28, 2014 as DOI: 10.1124/jpet.114.218644
This article has not been copyedited and formatted. The final version may differ from this version.

Endothelial cell capillary-like tube formation assay

The tube formation assay was conducted as described previously (Lee et al., 1999). Briefly, each well of a 48-well plate was coated with 80 μL of growth factor reduced-Matrigel and incubated at 37°C for polymerization. HUVECs were trypsinized and suspended in either EGM-2 medium or angiogenesis stimulation medium. Various concentrations of PAT were added to the cells for 1 h at 37°C before seeding. Cells were then plated onto the Matrigel layer at a density of 4-6×10^4 cells per well for 4-6 h. Cells with tube networks were visualized with 2 μg/mL calcein-AM using an Olympus fluorescence microscope (magnification of 64×). Three independent experiments were performed.

***In vivo* Matrigel plug assay**

The Matrigel plug assay was performed as described previously (Pyun et al., 2008). Briefly, 0.5 mL of Matrigel in the presence or absence of 60 ng of VEGF, 20 units of heparin and indicated concentrations of PAT (15 μmol/L and 50 μmol/L) was s.c. injected into the ventral area of 6-week-old C57BL/6 mice (*n*=6). After one week, the mice were sacrificed and the plugs were removed. The plugs were then fixed and embedded. For identification of the infiltration of newly formed endothelial cells, a von Willebrand factor (vWF) antibody (Chemicon, Temecula, CA) was used for immunohistochemistry. Images of neovasculature were taken using a Leica DM 4000B photo microscope (Solms, Germany; magnification of 400×).

Phospho-receptor tyrosine kinase analysis

Downloaded from jpet.aspetjournals.org at ASPET Journals on April 17, 2024

JPET Fast Forward. Published on October 28, 2014 as DOI: 10.1124/jpet.114.218644
This article has not been copyedited and formatted. The final version may differ from this version.

The human RTK phosphorylation antibody array was used according to the manufacturer's protocol. Briefly, membranes with 71 distinct RTKs were blocked for 1 h with gentle shaking. Cells were harvested using a cell scraper and lysed in modified radioimmunoprecipitation (RIPA) buffer (20 mmol/L Tris, 2.5 mmol/L EDTA, 1% TritonX-100, 1% deoxycholate, 0.1% SDS, 40 mmol/L NaF, 10 mmol/L $Na4P_2O_7$, and 1 mmol/L phenylmethylsulfonyl fluoride) supplemented with a phosphatase and protein inhibitor cocktail (Calbiochem; San Diego, CA). The lysates were gently rocked at 4°C for 30 min and centrifuged at 14,000 × g for 15 min. The sample protein concentrations were quantified using a micro BCA protein assay kit (Pierce Biotechnology, Rockford, IL). Lysates with 500 μg of total protein were subjected to the membranes at 4°C. Membranes were then incubated with biotin-conjugated antibodies and exposed to an enzyme horseradish peroxidase-conjugated streptavidin. The signals were visualized by the Li-Cor Odyssey Infrared system (LI-COR Biosciences, Lincoln, Nebraska).

Western blot analysis.

To determine the effects of PAT on the angiogenesis signaling cascade, HUVECs were first starved in serum-free EGM-2 for 10 h and then pretreated with or without various concentrations of PAT followed by stimulation with angiogenesis stimulation medium for 2-30 min. The whole-cell extracts were prepared in RIPA buffer. Approximately 40-50 μg of cellular protein from each treatment was applied to 6-8% SDS-polyacrylamide gels and transferred onto nitrocellulose membranes (Millipore, Billerica, MA). Membranes were incubated overnight with primary antibodies

Downloaded from jpet.aspetjournals.org at ASPET Journals on April 17, 2024

JPET Fast Forward. Published on October 28, 2014 as DOI: 10.1124/jpet.114.218644
This article has not been copyedited and formatted. The final version may differ from this version.

followed by incubation with fluorescent secondary antibodies (1/10,000; Sigma). After several washes, the signals were detected by the Li-Cor Odyssey Infrared system.

Statistical analysis

The statistical tests were carried out using Microsoft Excel and GraphPad Prism Software (version 5.0).Comparisons between groups were performed using one-way ANOVA followed by Student's *t* test. Data were presented as means ± standard deviation. *P*-values less than 0.05 were considered statistically significant (**P*<0.05; ***P*<0.01; ****P*<0.001).

Downloaded from jpet.aspetjournals.org at ASPET Journals on April 17, 2024

JPET Fast Forward. Published on October 28, 2014 as DOI: 10.1124/jpet.114.218644
This article has not been copyedited and formatted. The final version may differ from this version.

Results

PAT exerts cytotoxicity directly towards HUVECs

Chong and colleagues successfully repurposed the antifungal drug, itraconazole, as a potent angiogenesis inhibitor (Chong et al., 2007). Currently, there are several active clinical trials evaluating itraconazole as a cancer therapeutic agent (Nacev et al., 2011). Here, we applied a systematical screening by comparing differential sensitivities of endothelial cells and various NSCLC cells to 1280 chemical compounds approved by the FDA. We found that HUVECs were extremely susceptible to 4 drugs, including PAT, dactinomycin, thimerosal and phenylmercuric acetate compared with NSCLC cells (data not shown). In this article, we selected the antiparasitic agent, PAT, as a potential antiangiogenic candidate for further evaluation.

PAT selectively inhibited the growth of endothelial cells, but it had little direct anti-proliferative activity towards a panel of NSCLC cells with distinct molecular characteristics, including A549, PC9, NCI-H460, NCI-H441, NCI-H522, and NCI-H661 cells. As shown in Table 1, the IC_{50} of PAT in endothelial cells was approximately 4.32 μmol/L, which was at least 10-fold less than that in NSCLC cells, suggesting that PAT possessed relatively specific and directional cytotoxicity toward endothelial cells. To further evaluate the specificity of the inhibitory activities of PAT on activated endothelial cells, we examined its efficacy under three types of angiogenic stimuli, including EGM-2 (containing multiple growth factors), VEGF and

Downloaded from jpet.aspetjournals.org at ASPET Journals on April 17, 2024

JPET Fast Forward. Published on October 28, 2014 as DOI: 10.1124/jpet.114.218644
This article has not been copyedited and formatted. The final version may differ from this version.

bFGF. Our results showed that PAT exhibited equipotent inhibition of endothelial cell growth under these stimuli conditions, thus indicating that the agent might target the common growth factor-mediated angiogenesis signaling pathway.

The A549 and NCI-H441 cancer cells were highly resistant to PAT as their IC_{50} values were not measurable below the maximum tested concentration of 100 μmol/L. To avoid the concern of direct inhibition of PAT on tumor cells *in vivo*, we conducted a tumor xenograft mouse model using PAT-resistant A549 lung cancer cells.

PAT inhibits the growth of NSCLC cells either as a single agent or in combination with cisplatin chemotherapy

To investigate the *in vivo* anticancer effects of PAT, we established two types of xenograft mouse models. One type was constructed by PAT-resistant A549 (*KRAS* mut) lung cancer cells, and the other type used patient primary tumors. It is generally agreed that the patient-derived primary xenograft mouse model is the most favorable preclinical model for drug discovery as the explants of these models are biologically stable. The primary NSCLC tumors we used in this study represented adenocarcinoma with a *KRAS* mutation in codon 12 (a GGT→GAT transversion; Gly to Asp). Mice bearing established progressive tumor xenografts were i.p. administered daily with PAT at a dose of 40 mg/kg. Our results showed that administration of PAT significantly decreased the tumor growth rates of both xenografts (Fig. 1A and Fig. 1B). Compared with the vehicle group at the end of the treatment, single-agent therapy with PAT in A549 tumors and primary tumors resulted in 46.8 and 42.2%

Downloaded from jpet.aspetjournals.org at ASPET Journals on April 17, 2024

JPET Fast Forward. Published on October 28, 2014 as DOI: 10.1124/jpet.114.218644
This article has not been copyedited and formatted. The final version may differ from this version.

inhibition of tumor volume ($P < 0.05$) as well as 49.4 and 43.0% inhibition of tumor weight ($P < 0.05$), respectively. Such inhibitory effect of PAT was comparable to that of cisplatin monotherapy. When comparing with either single-agent therapy, addition of PAT to the cisplatin regimen resulted in a dramatic tumor growth inhibition. The combinational regimen led to 68.1% inhibition of tumor volumes in A549 tumors ($P < 0.001$) and 82.71% inhibition of tumor volumes in patient primary tumors ($P < 0.001$), suggesting a potent and synergistic anticancer action. The effect of combination therapy was quiet durable as it was maintained throughout the therapy period.

To further evaluate the health status of mice treated with PAT, the average body weight of mice was monitored every other day throughout the entire experiment. Our results showed that no obvious differences were found in mouse body weight among the PAT-treated groups and the control group. In contrast, the body weight of mice treated with cisplatin was marginally decreased ($P>0.05$). Furthermore, no adverse effects in other gross measures, such as skin ulcerations or toxic death, were observed in PAT-treated groups. These data provided an indication that PAT is safe at the tested dose and that the inhibition of tumor growth by PAT is not attributable to systemic toxicity.

PAT inhibits tumor angiogenesis *in vivo*

CD31 has been used as a biomarker of angiogenesis as it is constitutively expressed on the surface of the vascular endothelium (Takahama et al., 1999). Analysis of CD31 immunofluorescence staining of the tissue sections showed a

Downloaded from jpet.aspetjournals.org at ASPET Journals on April 17, 2024

JPET Fast Forward. Published on October 28, 2014 as DOI: 10.1124/jpet.114.218644
This article has not been copyedited and formatted. The final version may differ from this version.

significant reduction of tumor microvessel density in PAT-treated A549 and patient primary tumors (Fig. 2A). When compared with therapy involving cisplatin alone, addition of PAT to a cisplatin regimen (4 mg/kg every 7 days) resulted in enhanced inhibition of the tumor vasculature indicated by CD31-positive endothelial cells (green).

To further investigate the antiproliferative activity of PAT on lung cancer tumors *in vivo*, we directly analyzed the expression of Ki-67 protein by immunohistochemistry (Fig. 2B). In comparison with the vehicle treatment, PAT monotherapy led to 40.9 and 46% inhibition of Ki-67-positive cells in A549 tumors and in patient tumors, respectively. Addition of PAT to the combinational regimen resulted in the reduction of Ki-67 expression to 31.4% (P<0.001) and 19.5% (P<0.001) in A549 tumors and in patient primary tumors, respectively, suggesting a synergistic effect of CDDP and PAT *in vivo*. Given the synergistic effect of CDDP and PAT in anti-angiogenesis *in vivo*, we also evaluated the combinational effect of PAT and cisplatin in HUVECs *in vitro*. The results showed that the combination indexes under 50%, 75% and 90% effective dose were all less than 1, indicating a synergistic effect between these two drugs (Supplemental Figure 1). This data was well consistent with the potent and synergistic anticancer action of PAT and cisplatin in the tumor xenograft models.

PAT potently inhibits chemotactic migration of HUVECs *in vitro*

Endothelial cell migration is an important process in angiogenesis and

Downloaded from jpet.aspetjournals.org at ASPET Journals on April 17, 2024

JPET Fast Forward. Published on October 28, 2014 as DOI: 10.1124/jpet.114.218644
This article has not been copyedited and formatted. The final version may differ from this version.

functionally differs from proliferation (Lamalice et al., 2007). The effects of PAT on the chemotactic motility of HUVECs were assessed by wound-healing migration and Transwell assays. Compared to basal medium, EGM-2 with multiple growth factors triggered cell motility, but this effect was dose-dependently inhibited by PAT. The minimal effective action of PAT was observed at an approximate concentration of 1 μmol/L (Fig. 3A). In the Boyden chamber assay, we applied different stimuli to evaluate the inhibitory effects of PAT on HUVEC migration. PAT exhibited equipotent suppression of endothelial cell motility in EGM-2-, VEGF- and bFGF-stimulated conditions (Fig. 3B). In the Boyden chamber assay, 1 μmol/L PAT led to significant inhibition of endothelial cell migration, which was much less than its IC_{50} value of 2.5 μmol/L, indicating that cell motility was the primary target of PAT. During the treatment periods of migration assays, PAT even at 10 μmol/L had no obvious toxic effect on endothelial cell viability (Supplemental Figure 2)

PAT inhibits capillary-like structure formation of endothelial cells

Although angiogenesis is a complex process, tube formation is one of the key steps (Montesano et al., 1983). To investigate the potential effects of PAT on HUVEC tube formation, we conducted a 2-dimensional Matrigel assay. When HUVECs were placed on the growth factor–reduced Matrigel, elongated, cross-linked and robust tube-like structures were formed in the presence of VEGF, bFGF, and EGM-2 stimuli (Fig. 4). Incubation with indicated concentrations of PAT, tubular structure formation was inhibited in a dose-dependent manner. PAT exhibited a similar degree of potency for inhibition across all stimuli as shown in the HUVEC proliferation and chemotactic

Downloaded from jpet.aspetjournals.org at ASPET Journals on April 17, 2024

JPET Fast Forward. Published on October 28, 2014 as DOI: 10.1124/jpet.114.218644
This article has not been copyedited and formatted. The final version may differ from this version.

migration assays. The most effective concentration of PAT was around 2.5 μmol/L.

PAT inhibits VEGF-associated angiogenesis *in vivo*

To better characterize the inhibitory function of PAT on VEGF-induced angiogenesis *in vivo*, we utilized the mouse Matrigel plug assay. After being embedded s.c. into 6-week-old C57BL/6 mice for 7 days, plugs containing VEGF alone appeared dark red (Fig. 5A), indicating that infiltrating neovasculature had formed inside the Matrigel *via* angiogenesis. In contrast, the addition of different concentrations of PAT significantly inhibited neovascular formation. As indicated by the color of the plugs, the Matrigel plugs containing VEGF plus 10 μmol/L PAT were dramatically pale, indicating maximal inhibition of blood vessel formation.

Immunohistochemistry with the vWF antibody showed that infiltrating endothelial cells in PAT-treated groups were much less than those in the control group (embedded with equal amount of PBS) (Fig. 5B). These results suggested that PAT dramatically suppresses angiogenesis *in vivo*.

PAT inhibits the activation of key pro-angiogenic kinases

We further delineated the underlying mechanism of the antiangiogenesis effects of PAT. As shown in Fig. 6A, analysis of phospho-RTKs in treated HUVECs revealed that PAT suppressed the activation of multiple critical receptors primarily contributing to angiogenesis, including VEGFR2, FGFR1, FGFR2, Tie2 and ErbB2. None of the other RTKs present on the protein array were similarly affected. To validate this result, we further confirmed the inhibition of PAT on the activation of VEGFR2. As shown in

Downloaded from jpet.aspetjournals.org at ASPET Journals on April 17, 2024

JPET Fast Forward. Published on October 28, 2014 as DOI: 10.1124/jpet.114.218644
This article has not been copyedited and formatted. The final version may differ from this version.

figure 6B, PAT at the same concentration strongly inhibited VEGF-activated VEGFR2 phosphorylation (at both sites of Tyr 1175 and Tyr 996). To test if PAT blocked the activation of the RTKs by interfering with their total protein levels, we utilized the whole cellular protein from the treated HUVECs in Western blotting analyses. As indicated, PAT had little effect on the expression levels of VEGFR2 and Tie2 in HUVECs even when the HUVECs were exposed to PAT for 48 h (Fig. 6C).

We further examined whether PAT successively inhibited the intracellular signaling molecules downstream of the RTKs, and found that PAT dose-dependently suppressed the phosphorylation of Src and FAK triggered by VEGF [50 ng/mL; (***i***)], bFGF [50 ng/mL; (***ii***)] and Angiogenin-1 [200 ng/mL; (***iii***)] in HUVECsat concentrations ranging from 2.5 to 5 μmol/L (Fig. 6D). In addition, PAT inhibited the activation of the Src/FAK pathway in a time-dependent manner (Supplemental Figure 3). Notably, these effects were specific because the phosphorylation of AKT and ERK was not detectably affected by PAT under the same treatment.

Downloaded from jpet.aspetjournals.org at ASPET Journals on April 17, 2024

JPET Fast Forward. Published on October 28, 2014 as DOI: 10.1124/jpet.114.218644
This article has not been copyedited and formatted. The final version may differ from this version.

Discussion

Although targeted therapy for cancer has been significantly advanced, cancer remains to be one of the leading causes of mortality worldwide. During the last decade, pharmaceutical industries have increased their research spending. However, it is estimated that only 0.01% of prospective anticancer agents receive FDA approval and that only 5% of oncology drugs entering into Phase I clinical trials are ultimately approved. As various diseases stem from a common molecular basis and share similar targets of the cells, repurposing established drugs is rationally considered and has gained attention over the past years (Gupta et al., 2013). Through genomics, proteomics, and informatics technologies, researchers have characterized many non-cancer drugs for their anti-cancerous activities, and most of these repurposed drugs show promising anticancer efficacy in the clinic. The successful re-profiling of thalidomide is an example. Thalidomide, which was originally used as a sedative hypnotic and withdrawn from the market due to teratogenesis induction, exhibits potent properties against several malignancies through regulating numerous cancer-related signaling pathways. This drug was finally approved by the FDA for treating patients with multiple myeloma because of its antiangiogenic (D'Amato et al., 1994) and oxidative DNA-damaging properties (Parman et al., 1999).

Cancer-associated angiogenesis contributes to the growth and progression of solid tumors and remains a primary target for anticancer drug development (Kerbel, 2008; Cook and Figg, 2010). Based on the hypothesis of clinical drug indication switching, we performed screening of existing drugs against tumor angiogenesis. Our screening

Downloaded from jpet.aspetjournals.org at ASPET Journals on April 17, 2024

JPET Fast Forward. Published on October 28, 2014 as DOI: 10.1124/jpet.114.218644
This article has not been copyedited and formatted. The final version may differ from this version.

strategy by analyzing the cytotoxicity of established drugs in various NSCLC cells and HUVECs differed from the reported workflow (Chong et al., 2007) in that only endothelial cells were applied to the initial screening. By comparison of the IC_{50} values, we described PAT as a novel agent with antiangiogenic potential. Using *in vitro* and *in vivo* angiogenesis assays, we reported for the first time that PAT effectively inhibits angiogenesis and tumor growth of NSCLC.

Angiogenesis is the summation of multiple cellular and biologic processes to propagate existing blood vessels. In this study, we evaluated the effect of PAT on multiple steps of endothelial cell function. In HUVEC viability assays, PAT consistently exhibited potent antiproliferative activities, and the potency was comparable in response to different stimuli. Moreover, the growth inhibition of PAT was cell-type specific as the agent showed modest effects at even higher concentrations on NSCLC cells harboring different molecular characteristics. Based on this observation, we postulate that vascular endothelial cells may be the primary target of PAT rather than the surrounding tumor cells in tumor microenvironments. Additionally, at concentrations of 1-2.5 μmol/L, PAT was sufficient to inhibit endothelial chemotaxis and tube formation, but the effective inhibitory concentration of PAT on endothelial cell proliferation was relatively higher, thereby suggesting that the molecules involved in cell motility, skeleton and differentiation were the principal targets of PAT. Novel angiogenesis therapies are being developed to target receptor tyrosine kinases (RTKs) (Wozniak, 2012). Evaluating the phosphorylation status of RTKs showed that PAT had the capacity to suppress the activation of multiple critical

Downloaded from jpet.aspetjournals.org at ASPET Journals on April 17, 2024

JPET Fast Forward. Published on October 28, 2014 as DOI: 10.1124/jpet.114.218644
This article has not been copyedited and formatted. The final version may differ from this version.

receptor kinases (VEGFR2, FGFR1, FGFR2, Tie2 and ErbB2) involved in angiogenesis. We confirmed that this inhibition mediated by PAT was not associated with the reduction RTK protein levels, which differed from itraconazole (antifungal drug) that inhibited VEGFR2 glycosylation and trafficking (Nacev et al., 2011). PAT at a lower concentration of 2.5 μmol/L effectively inhibited the RTK-triggered Src and FAK activation in endothelial cells, but had little effect on the activation of AKT and ERK, thereby indicating the specificity of PAT on cellular signaling intervention. The nonreceptor tyrosine kinase, Src, directly interacts or cooperates with RTKs, including epithelial growth factor receptor and VEGFR2, as well as G protein–coupled receptors, integrins, actins, GTPase-activating proteins and FAK. These interactions are mainly involved in the regulation of cell shape, motility and differentiation. In agreement with the above results, the motility of endothelial cells triggered by different stimuli was significantly inhibited by PAT at lower concentrations, suggesting that Src/FAK signaling is a rational molecular target of PAT in angiogenesis. The repression of Src/FAK signaling leads to a downregulation of growth factor expression (Kanda et al., 2007; Kim et al., 2009). Thus, we assumed that PAT might also block the production of pro-angiogenic molecules released from tumor cells. Considering the potency of PAT on cell motility by blocking Src and FAK kinases, its direct action on tumor metastasis should be further studied. Additionally, it has been addressed recently that Src is a common signaling node downstream of multiple trastuzumab-resistant pathways (Zhang et al., 2011), and Src-targeting regimens are proposed as the novel strategy to treat patients with breast cancer

Downloaded from jpet.aspetjournals.org at ASPET Journals on April 17, 2024

JPET Fast Forward. Published on October 28, 2014 as DOI: 10.1124/jpet.114.218644
This article has not been copyedited and formatted. The final version may differ from this version.

suffering from metastasis. Given that PAT specifically affects the Src/FAK complex, this agent may be a constituent in combination with trastuzumab in the treatment of tumor metastasis.

Initial study has demonstrated that PAT, like As_2O_3, may inhibit acute promyelocytic leukemia *in vitro* (Lecureur et al., 2002a; Lecureur et al., 2002b). In this study, we reported for the first time that PAT also exerted anticancer properties in solid tumors. In addition to the *in vitro* assays, we conducted two representative tumor xenograft models to illustrate the antitumor efficacy of PAT *in vivo*. Our *in vivo* results strengthened the antiangiogenesis data for PAT as evidenced by CD31 immunofluorescence. In addition to A549 tumors, we additionally set up patient-derived primary tumor xenograft models, which have explants that are biologically stable when passaged in mice in terms of global gene expression patterns, mutational status, tumor architecture, and drug responsiveness. In both of the *in vivo* models, PAT presented significant inhibition of tumor volume and tumor weight as a single agent. When combined with the chemotherapy drug, cisplatin, PAT contributed to a durable cytostatic tumor growth response, thereby suggesting a synergistic property. As one of the first chemotherapeutic agents used in the treatment of leishmaniasis, PAT was abandoned because of its toxicity. In our preclinical cancer *in vivo* models, PAT did not show any gross toxicity at the tested dosage, suggesting that PAT may be clinically safe in NSCLC treatment. Importantly, PAT concentrations acting on endothelial cells were less than 10 μmol/L, and such concentrations are likely to be achievable *in vivo* in humans.

Downloaded from jpet.aspetjournals.org at ASPET Journals on April 17, 2024

JPET Fast Forward. Published on October 28, 2014 as DOI: 10.1124/jpet.114.218644
This article has not been copyedited and formatted. The final version may differ from this version.

In the current cancer treatment for NSCLC, EGFR inhibitors (e.g., gefitinib and erlotinib), have been applied into clinics as first-line drugs. However, tumors harboring *KRAS* mutations inevitably result in intrinsic resistance to EGFR inhibitor-based therapy (Massarelli et al., 2007). Unfortunately, no effective drug has been developed to treat this type of cancer with a *KRAS* mutation genotype. Importantly, the *in vivo* tumors we used in this study are all *KRAS* mutant NSCLC, and PAT effectively inhibited the tumor growth by blockade of tumor angiogenesis. Our findings have critical clinical implications for potential use of PAT as an efficient agent for *KRAS* mutant NSCLC.

Downloaded from jpet.aspetjournals.org at ASPET Journals on April 17, 2024

JPET Fast Forward. Published on October 28, 2014 as DOI: 10.1124/jpet.114.218644
This article has not been copyedited and formatted. The final version may differ from this version.

Authorship Contributions

Participate in research design: Wang, Yu, Guo, Lu, Liu, Pang

Conducted experiments: Wang, Yu, Guo, Jiang

Performed data analysis: Wang, Pang

Wrote or contributed to the writing of the manuscript: Wang, Pang

Downloaded from jpet.aspetjournals.org at ASPET Journals on April 17, 2024

JPET Fast Forward. Published on October 28, 2014 as DOI: 10.1124/jpet.114.218644
This article has not been copyedited and formatted. The final version may differ from this version.

References

Algire GH, Legallais FY and Anderson BF (1954) Vascular reactions of normal and malignant tissues in Vivo. VI. The role of hypotension in the action of components of podophyllin on transplanted sarcomas. *J Natl Cancer Inst* **14**:879-893.

Asahara T, Bauters C, Zheng LP, Takeshita S, Bunting S, Ferrara N, Symes JF and Isner JM (1995) Synergistic effect of vascular endothelial growth factor and basic fibroblast growth factor on angiogenesis in vivo. *Circulation* **92**:II365-371.

Chong CR and Sullivan DJ, Jr. (2007) New uses for old drugs. *Nature* **448**:645-646.

Chong CR, Xu J, Lu J, Bhat S, Sullivan DJ, Jr. and Liu JO (2007) Inhibition of angiogenesis by the antifungal drug itraconazole. *ACS Chem Biol* **2**:263-270.

Cook KM and Figg WD (2010) Angiogenesis inhibitors: current strategies and future prospects. *CA Cancer J Clin* **60**:222-243.

D'Amato RJ, Loughnan MS, Flynn E and Folkman J (1994) Thalidomide is an inhibitor of angiogenesis. *Proc Natl Acad Sci U S A* **91**:4082-4085.

Downward J (2003) Targeting RAS signalling pathways in cancer therapy. *Nat Rev Cancer* **3**:11-22.

Ferrara N, Hillan KJ, Gerber HP and Novotny W (2004) Discovery and development of bevacizumab, an anti-VEGF antibody for treating cancer. *Nat Rev Drug Discov* **3**:391-400.

Ferrara N and Kerbel RS (2005) Angiogenesis as a therapeutic target. *Nature*

Downloaded from jpet.aspetjournals.org at ASPET Journals on April 17, 2024

JPET Fast Forward. Published on October 28, 2014 as DOI: 10.1124/jpet.114.218644
This article has not been copyedited and formatted. The final version may differ from this version.

438:967-974.

Folkman J (1971) Tumor angiogenesis: therapeutic implications. *N Engl J Med* **285**:1182-1186.

Guba M, von Breitenbuch P, Steinbauer M, Koehl G, Flegel S, Hornung M, Bruns CJ, Zuelke C, Farkas S, Anthuber M, Jauch KW and Geissler EK (2002) Rapamycin inhibits primary and metastatic tumor growth by antiangiogenesis: involvement of vascular endothelial growth factor. *Nat Med* **8**:128-135.

Gupta SC, Sung B, Prasad S, Webb LJ and Aggarwal BB (2013) Cancer drug discovery by repurposing: teaching new tricks to old dogs. *Trends Pharmacol Sci* **34**:508-517.

Hanahan D and Folkman J (1996) Patterns and emerging mechanisms of the angiogenic switch during tumorigenesis. *Cell* **86**:353-364.

Jeltsch M, Leppanen VM, Saharinen P and Alitalo K (2013) Receptor tyrosine kinase-mediated angiogenesis. *Cold Spring Harb Perspect Biol* **5**.

Jones MK, Wang H, Peskar BM, Levin E, Itani RM, Sarfeh IJ and Tarnawski AS (1999) Inhibition of angiogenesis by nonsteroidal anti-inflammatory drugs: insight into mechanisms and implications for cancer growth and ulcer healing. *Nat Med* **5**:1418-1423.

Kanda S, Miyata Y, Kanetake H and Smithgall TE (2007) Non-receptor protein-tyrosine kinases as molecular targets for antiangiogenic therapy (Review). *Int J Mol Med* **20**:113-121.

Kerbel RS (2008) Tumor angiogenesis. *N Engl J Med* **358**:2039-2049.

Downloaded from jpet.aspetjournals.org at ASPET Journals on April 17, 2024

JPET Fast Forward. Published on October 28, 2014 as DOI: 10.1124/jpet.114.218644
This article has not been copyedited and formatted. The final version may differ from this version.

Kim LC, Song L and Haura EB (2009) Src kinases as therapeutic targets for cancer. *Nat Rev Clin Oncol* **6**:587-595.

Lamalice L, Le Boeuf F and Huot J (2007) Endothelial cell migration during angiogenesis. *Circ Res* **100**:782-794.

Lecureur V, Lagadic-Gossmann D and Fardel O (2002a) Potassium antimonyl tartrate induces reactive oxygen species-related apoptosis in human myeloid leukemic HL60 cells. *Int J Oncol* **20**:1071-1076.

Lecureur V, Le Thiec A, Le Meur A, Amiot L, Drenou B, Bernard M, Lamy T, Fauchet R and Fardel O (2002b) Potassium antimonyl tartrate induces caspase- and reactive oxygen species-dependent apoptosis in lymphoid tumoral cells. *Br J Haematol* **119**:608-615.

Lee OH, Kim YM, Lee YM, Moon EJ, Lee DJ, Kim JH, Kim KW and Kwon YG (1999) Sphingosine 1-phosphate induces angiogenesis: its angiogenic action and signaling mechanism in human umbilical vein endothelial cells. *Biochem Biophys Res Commun* **264**:743-750.

Lemmon MA and Schlessinger J (2010) Cell signaling by receptor tyrosine kinases. *Cell* **141**:1117-1134.

Liu P, Cheng H, Roberts TM and Zhao JJ (2009) Targeting the phosphoinositide 3-kinase pathway in cancer. *Nat Rev Drug Discov* **8**:627-644.

Lund EL, Spang-Thomsen M, Skovgaard-Poulsen H and Kristjansen PE (1998) Tumor angiogenesis--a new therapeutic target in gliomas. *Acta Neurol Scand* **97**:52-62.

Downloaded from jpet.aspetjournals.org at ASPET Journals on April 17, 2024

JPET Fast Forward. Published on October 28, 2014 as DOI: 10.1124/jpet.114.218644
This article has not been copyedited and formatted. The final version may differ from this version.

Massarelli E, Varella-Garcia M, Tang X, Xavier AC, Ozburn NC, Liu DD, Bekele BN, Herbst RS and Wistuba, II (2007) KRAS mutation is an important predictor of resistance to therapy with epidermal growth factor receptor tyrosine kinase inhibitors in non-small-cell lung cancer. *Clin Cancer Res* **13**:2890-2896.

McLean GW, Carragher NO, Avizienyte E, Evans J, Brunton VG and Frame MC (2005) The role of focal-adhesion kinase in cancer - a new therapeutic opportunity. *Nat Rev Cancer* **5**:505-515.

Migliardi G, Sassi F, Torti D, Galimi F, Zanella ER, Buscarino M, Ribero D, Muratore A, Massucco P, Pisacane A, Risio M, Capussotti L, Marsoni S, Di Nicolantonio F, Bardelli A, Comoglio PM, Trusolino L and Bertotti A (2012) Inhibition of MEK and PI3K/mTOR suppresses tumor growth but does not cause tumor regression in patient-derived xenografts of RAS-mutant colorectal carcinomas. *Clin Cancer Res* **18**:2515-2525.

Montesano R, Orci L and Vassalli P (1983) In vitro rapid organization of endothelial cells into capillary-like networks is promoted by collagen matrices. *J Cell Biol* **97**:1648-1652.

Nacev BA, Grassi P, Dell A, Haslam SM and Liu JO (2011) The antifungal drug itraconazole inhibits vascular endothelial growth factor receptor 2 (VEGFR2) glycosylation, trafficking, and signaling in endothelial cells. *J Biol Chem* **286**:44045-44056.

Niki T, Iba S, Tokunou M, Yamada T, Matsuno Y and Hirohashi S (2000) Expression of vascular endothelial growth factors A, B, C, and D and their relationships to

Downloaded from jpet.aspetjournals.org at ASPET Journals on April 17, 2024

JPET Fast Forward. Published on October 28, 2014 as DOI: 10.1124/jpet.114.218644
This article has not been copyedited and formatted. The final version may differ from this version.

lymph node status in lung adenocarcinoma. *Clin Cancer Res* **6**:2431-2439.

Pang X, Yi T, Yi Z, Cho SG, Qu W, Pinkaew D, Fujise K and Liu M (2009a) Morelloflavone, a biflavonoid, inhibits tumor angiogenesis by targeting rho GTPases and extracellular signal-regulated kinase signaling pathways. *Cancer Res* **69**:518-525.

Pang X, Yi Z, Zhang X, Sung B, Qu W, Lian X, Aggarwal BB and Liu M (2009b) Acetyl-11-keto-beta-boswellic acid inhibits prostate tumor growth by suppressing vascular endothelial growth factor receptor 2-mediated angiogenesis. *Cancer Res* **69**:5893-5900.

Parman T, Wiley MJ and Wells PG (1999) Free radical-mediated oxidative DNA damage in the mechanism of thalidomide teratogenicity. *Nat Med* **5**:582-585.

Paz-Ares LG, Biesma B, Heigener D, von Pawel J, Eisen T, Bennouna J, Zhang L, Liao M, Sun Y, Gans S, Syrigos K, Le Marie E, Gottfried M, Vansteenkiste J, Alberola V, Strauss UP, Montegriffo E, Ong TJ, Santoro A and Group NREUSIS (2012) Phase III, randomized, double-blind, placebo-controlled trial of gemcitabine/cisplatin alone or with sorafenib for the first-line treatment of advanced, nonsquamous non-small-cell lung cancer. *J Clin Oncol* **30**:3084-3092.

Presta M, Dell'Era P, Mitola S, Moroni E, Ronca R and Rusnati M (2005) Fibroblast growth factor/fibroblast growth factor receptor system in angiogenesis. *Cytokine Growth Factor Rev* **16**:159-178.

Pyun BJ, Choi S, Lee Y, Kim TW, Min JK, Kim Y, Kim BD, Kim JH, Kim TY, Kim

Downloaded from jpet.aspetjournals.org at ASPET Journals on April 17, 2024

JPET Fast Forward. Published on October 28, 2014 as DOI: 10.1124/jpet.114.218644
This article has not been copyedited and formatted. The final version may differ from this version.

YM and Kwon YG (2008) Capsiate, a nonpungent capsaicin-like compound, inhibits angiogenesis and vascular permeability via a direct inhibition of Src kinase activity. *Cancer Res* **68**:227-235.

Qian Y, Liu S, Guan Y, Pan H, Guan X, Qiu Z, Li L, Gao N, Zhao Y, Li X, Lu Y, Liu M and Li D (2013) Lgr4-mediated Wnt/beta-catenin signaling in peritubular myoid cells is essential for spermatogenesis. *Development* **140**:1751-1761.

Ranpura V, Hapani S and Wu S (2011) Treatment-related mortality with bevacizumab in cancer patients: a meta-analysis. *JAMA* **305**:487-494.

Saharinen P, Eklund L, Pulkki K, Bono P and Alitalo K (2011) VEGF and angiopoietin signaling in tumor angiogenesis and metastasis. *Trends Mol Med* **17**:347-362.

Sandler A, Gray R, Perry MC, Brahmer J, Schiller JH, Dowlati A, Lilenbaum R and Johnson DH (2006) Paclitaxel-carboplatin alone or with bevacizumab for non-small-cell lung cancer. *N Engl J Med* **355**:2542-2550.

Schulert AR, Rassoul AA, Mansour M, Girgis N, McConnell E and Farid Z (1966) Biological disposition of antibilharzial antimony drugs. II. Antimony fate and uptake by Schistosoma haematobium eggs in man. *Exp Parasitol* **18**:397-402.

Sennino B and McDonald DM (2012) Controlling escape from angiogenesis inhibitors. *Nat Rev Cancer* **12**:699-709.

Siegel R, DeSantis C, Virgo K, Stein K, Mariotto A, Smith T, Cooper D, Gansler T, Lerro C, Fedewa S, Lin C, Leach C, Cannady RS, Cho H, Scoppa S, Hachey M, Kirch R, Jemal A and Ward E (2012) Cancer treatment and survivorship

Downloaded from jpet.aspetjournals.org at ASPET Journals on April 17, 2024

JPET Fast Forward. Published on October 28, 2014 as DOI: 10.1124/jpet.114.218644
This article has not been copyedited and formatted. The final version may differ from this version.

statistics, 2012. *CA Cancer J Clin* **62**:220-241.

Siegel R, Naishadham D and Jemal A (2013) Cancer statistics, 2013. *CA Cancer J Clin* **63**:11-30.

Takahama M, Tsutsumi M, Tsujiuchi T, Nezu K, Kushibe K, Taniguchi S, Kotake Y and Konishi Y (1999) Enhanced expression of Tie2, its ligand angiopoietin-1, vascular endothelial growth factor, and CD31 in human non-small cell lung carcinomas. *Clin Cancer Res* **5**:2506-2510.

Wozniak A (2012) Challenges in the current antiangiogenic treatment paradigm for patients with non-small cell lung cancer. *Crit Rev Oncol Hematol* **82**:200-212.

Zhang S, Huang WC, Li P, Guo H, Poh SB, Brady SW, Xiong Y, Tseng LM, Li SH, Ding Z, Sahin AA, Esteva FJ, Hortobagyi GN and Yu D (2011) Combating trastuzumab resistance by targeting SRC, a common node downstream of multiple resistance pathways. *Nat Med* **17**:461-469.

Downloaded from jpet.aspetjournals.org at ASPET Journals on April 17, 2024

JPET Fast Forward. Published on October 28, 2014 as DOI: 10.1124/jpet.114.218644
This article has not been copyedited and formatted. The final version may differ from this version.

Footnotes

This work is supported by grants from National Basic Research Program of China [Grant 2012CB910401], National Natural Science Foundation of China [Grants 81101683, 81402482, 30930055 and 31271468], the Science and Technology Commission of Shanghai Municipality [Grants 12XD1406100, 12ZR1408700 and 11DZ2260300], the Chenguang Program from Shanghai Municipal Education Commission [Grant 10CG25], and the Fundamental Research Funds for the Central Universities [Grant 78260029].

Downloaded from jpet.aspetjournals.org at ASPET Journals on April 17, 2024

JPET Fast Forward. Published on October 28, 2014 as DOI: 10.1124/jpet.114.218644
This article has not been copyedited and formatted. The final version may differ from this version.

Legends for Figures

Figure 1. PAT potently retards tumor growth of NSCLC *in vivo*.

A. PAT inhibited A549 tumor growth as measured by tumor volume (*left*) and solid tumor weight (*middle*) and had little effect on the mouse body weight (*right*) at the tested dose. Mice bearing A549 tumors were treated with PBS, PAT (40 mg/kg; i.p.; daily), cisplatin (CDDP; 4 mg/kg; i.p.; once a week), or a combination of PAT and cisplatin (n=8 per group). ***B***. PAT suppressed the growth of patient primary NSCLC tumors. The patient primary NSCLC tumor xenograft mouse model was set up according to the protocol described in the ***Materials and Methods***. Individual groups of mice bearing patient primary tumors were subjected to different treatments. *Dots*, mean; *bars*, standard deviation;*, $P < 0.05$; **, $P < 0.01$; ***, $P < 0.001$ *vs.* the vehicle control group.

Figure 2. PAT inhibits angiogenesis and tumor cell proliferation in human NSCLC xenografts.

A. Antiangiogenic effects of PAT, CDDP, and a combination of PAT and CDDP as assessed by immunohistochemical analysis of CD31 (green) in mice implanted with A549 cells or human primary tumors. ***B***. Immunohistochemical analysis of Ki-67 staining in tumors (brown) from two types of human NSCLC xenograft mouse models. Representative CD31 or Ki-67 staining of lung tumors viewed at 200× magnification. Quantitative number of CD31-positive and Ki-67-positive cells was determined by manual counting in three random fields from six solid tumors of each group. *Columns*,

Downloaded from jpet.aspetjournals.org at ASPET Journals on April 17, 2024

JPET Fast Forward. Published on October 28, 2014 as DOI: 10.1124/jpet.114.218644
This article has not been copyedited and formatted. The final version may differ from this version.

mean; *bars*, standard deviation; **, $P < 0.01$ *vs*. control.

Figure 3. PAT potently inhibits endothelial cell migration and chemotaxis *in vitro.* ***A***. PAT inhibited HUVEC migration in a wound-healing assay. HUVECs were first synchronized by starvation. Confluent cells were then scratched and treated with EGM-2 media containing DMSO or 1, 2.5, 5, 10 μmol/L PAT. Migrating cells were stained by calcein-AM and quantified by manual counting. Magnification of 64×. ***B***. PAT inhibited migration of stimulated HUVECs in a Transwell assay. HUVECs ($4\text{-}5\times10^4$) were pretreated with PAT in EGM-2 containing 0.5% FBS for 30 min before seeding into the upper chambers. The bottom chamber was filled with EGM-2 basic media supplemented with EGM-2, 10 ng/mL VEGF, and 12 ng/mL bFGF. The HUVECs that migrated through the membrane were quantified. Magnification of 160×. *Columns*, mean from three different experiments with duplicates; *b*ars, SD. *, $P < 0.05$; ***, $P < 0.001$ *vs*. the DMSO group (EGM-2 alone, VEGF alone or bFGF alone).

Figure 4. **PAT inhibits the capillary-like structure formation in endothelial cells.** HUVECs stimulated with EGM-2, 10 ng/mL VEGF, or 12 ng/mL bFGF were allowed to spontaneously form tube networks after treatment with DMSO or indicated concentrations of PAT. After 4-6 h, the tubular networks were visualized with calcein-AM and photographed (magnification of 64×).

Downloaded from jpet.aspetjournals.org at ASPET Journals on April 17, 2024

JPET Fast Forward. Published on October 28, 2014 as DOI: 10.1124/jpet.114.218644
This article has not been copyedited and formatted. The final version may differ from this version.

Figure 5. PAT inhibits VEGF-stimulated angiogenesis *in vivo*.

Six-week-old C57BL/6 mice were injected with 500 μL of Matrigel containing indicated concentrations of PAT, 60 ng of VEGF, and 20 units of heparin into the ventral area (*n*=6 per group). After a week, the skin of mice was pulled back to expose the intact Matrigel plugs. ***A***. Matrigel plugs with different treatments were photographed. ***B***. Representative vWF staining of Matrigel plugs viewed at 400× magnification. The Matrigel plugs were fixed, sectioned and stained with the vWF antibody (magnification of 400×).

Figure 6. **PAT inhibits the activation of RTKs and the Src/FAK pathway in endothelial cells.**

A. PAT suppressed the expression of multiple RTKs in HUVECs. Cell lysates were generated from EGM-2–stimulated HUVECs treated with 15 μmol/L PAT or with DMSO for 24 h. Cell lysates was then centrifuged and hybridized to a human RTK phosphorylation antibody array. ***B***. PAT dramatically suppressed VEGF-mediated activation of VEGFR2. Proteins from different treatments were analyzed by Western blotting assay. ***C***. PAT had little effect on the expression levels of VEGFR2 and Tie2. ***D***. PAT inhibited the activation of the Src/FAK pathway but had little effect on the activation of AKT and ERK. Starved HUVECs were pretreated with or without various concentrations of PAT followed by stimulation with angiogenesis stimulation medium (50 ng/mL VEGF, 50 ng/mL bFGF or 200 ng/mL Ang-1) for 2-30 min. Proteins from different groups were analyzed by Western blotting analysis using

Downloaded from jpet.aspetjournals.org at ASPET Journals on April 17, 2024

JPET Fast Forward. Published on October 28, 2014 as DOI: 10.1124/jpet.114.218644
This article has not been copyedited and formatted. The final version may differ from this version.

specific antibodies.

Downloaded from jpet.aspetjournals.org at ASPET Journals on April 17, 2024

JPET Fast Forward. Published on October 28, 2014 as DOI: 10.1124/jpet.114.218644
This article has not been copyedited and formatted. The final version may differ from this version.

Tables

Table 1. The Cytotoxicity of PAT is Direct towards Endothelial Cells

	Cell lines	IC_{50} (μmol/L)
Human endothelial cells	HUVECs (EGM-2)	4.32
	HUVECs (VEGF)	7.55
	HUVECs (bFGF)	6.05
Human lung fibroblast cells	WI-38	>100
	MRC-5	49.72
Human lung cancer cells	A549	>100
	NCI-H441	>100
	NCI-H460	42.72
	PC9	72.52
	NCI-H522	44.68
	NCI-H661	67.87

Note. Growth inhibition of HUVECs, a panel of NSCLC cells and normal lung fibroblast cells by PAT as determined by MTS assay. The half inhibitory concentration (IC_{50}) values were shown.

Downloaded from jpet.aspetjournals.org at ASPET Journals on April 17, 2024

Figure 1

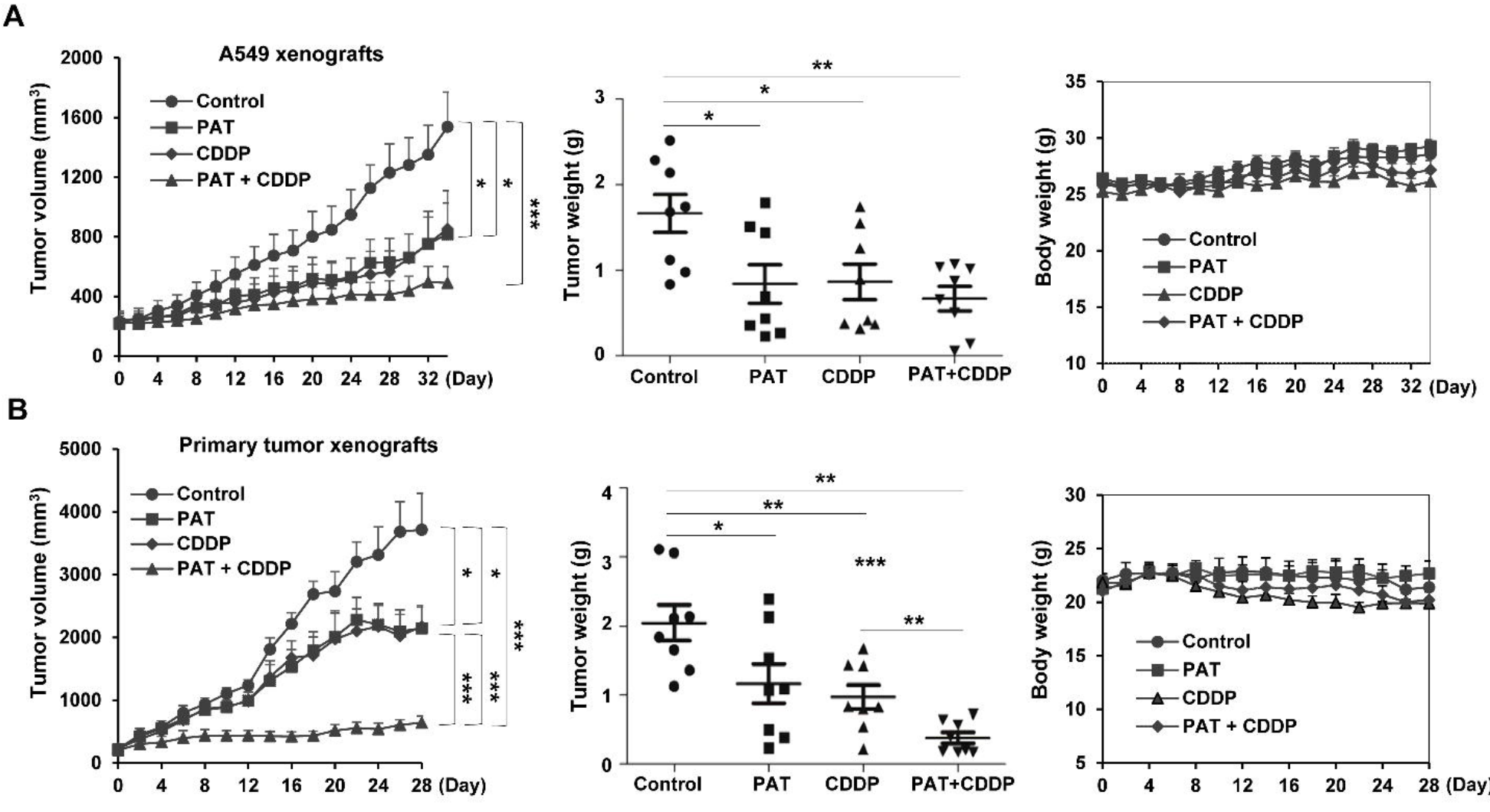
A
A549 xenografts
Tumor volume (mm³)
Control
PAT
CDDP
PAT + CDDP
0 4 8 12 16 20 24 28 32 (Day)
Tumor weight (g)
Control PAT CDDP PAT+CDDP
Body weight (g)
Control
PAT
CDDP
PAT + CDDP
0 4 8 12 16 20 24 28 32 (Day)
B
Primary tumor xenografts
Tumor volume (mm³)
Control
PAT
CDDP
PAT + CDDP
0 4 8 12 16 20 24 28 (Day)
Tumor weight (g)
Control PAT CDDP PAT+CDDP
Body weight (g)
Control
PAT
CDDP
PAT + CDDP
0 4 8 12 16 20 24 28 (Day)

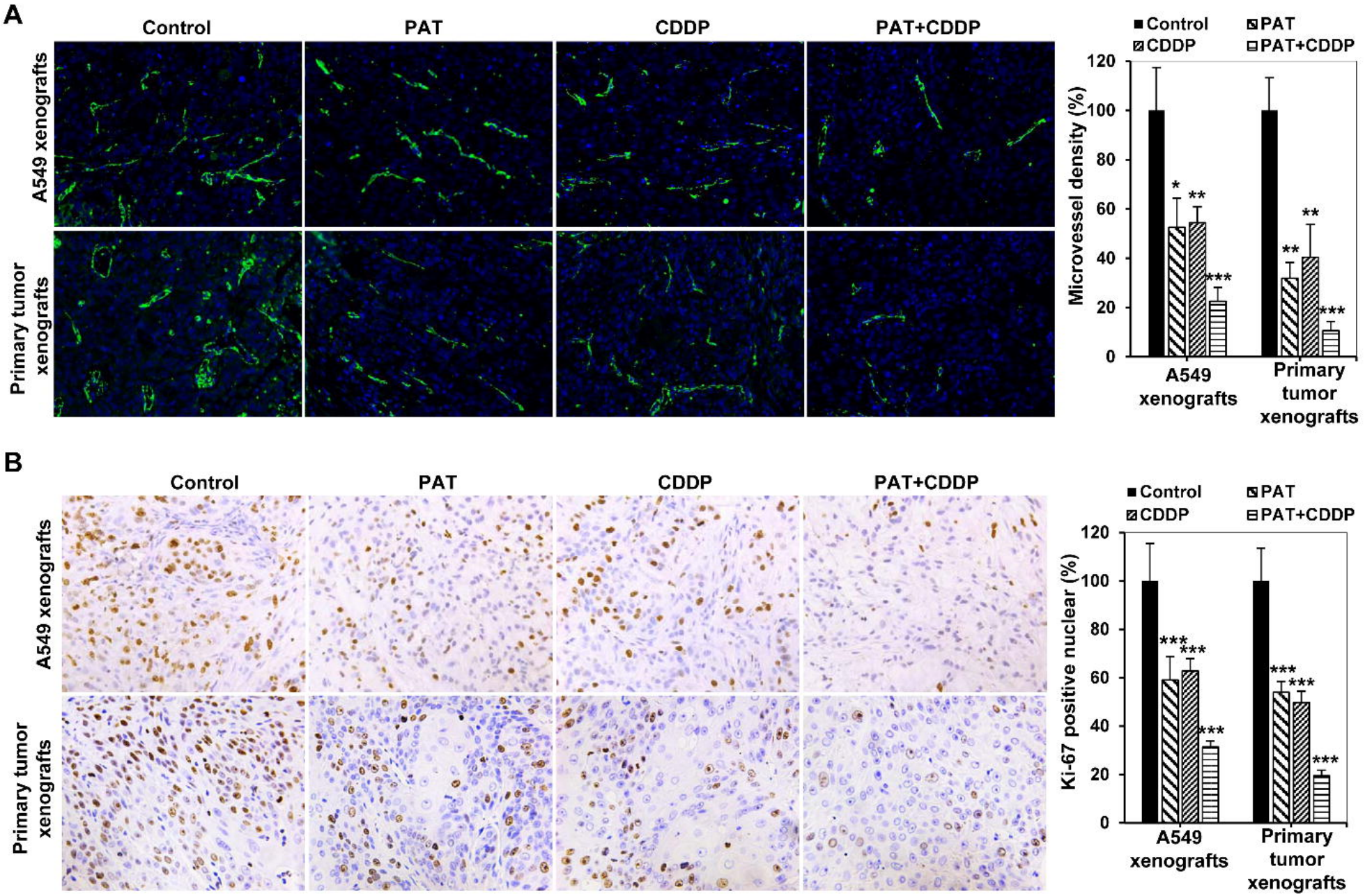
A
Control
PAT
CDDP
PAT+CDDP
A549 xenografts
Primary tumor xenografts
Control
PAT
CDDP
PAT+CDDP
Microvessel density (%)
120
100
80
60
40
20
0
*
**
***
**
**
***
A549 xenografts
Primary tumor xenografts
B
Control
PAT
CDDP
PAT+CDDP
A549 xenografts
Primary tumor xenografts
Control
PAT
CDDP
PAT+CDDP
Ki-67 positive nuclear (%)
120
100
80
60
40
20
0
***
***
***
***
***
***
A549 xenografts
Primary tumor xenografts

Figure 3

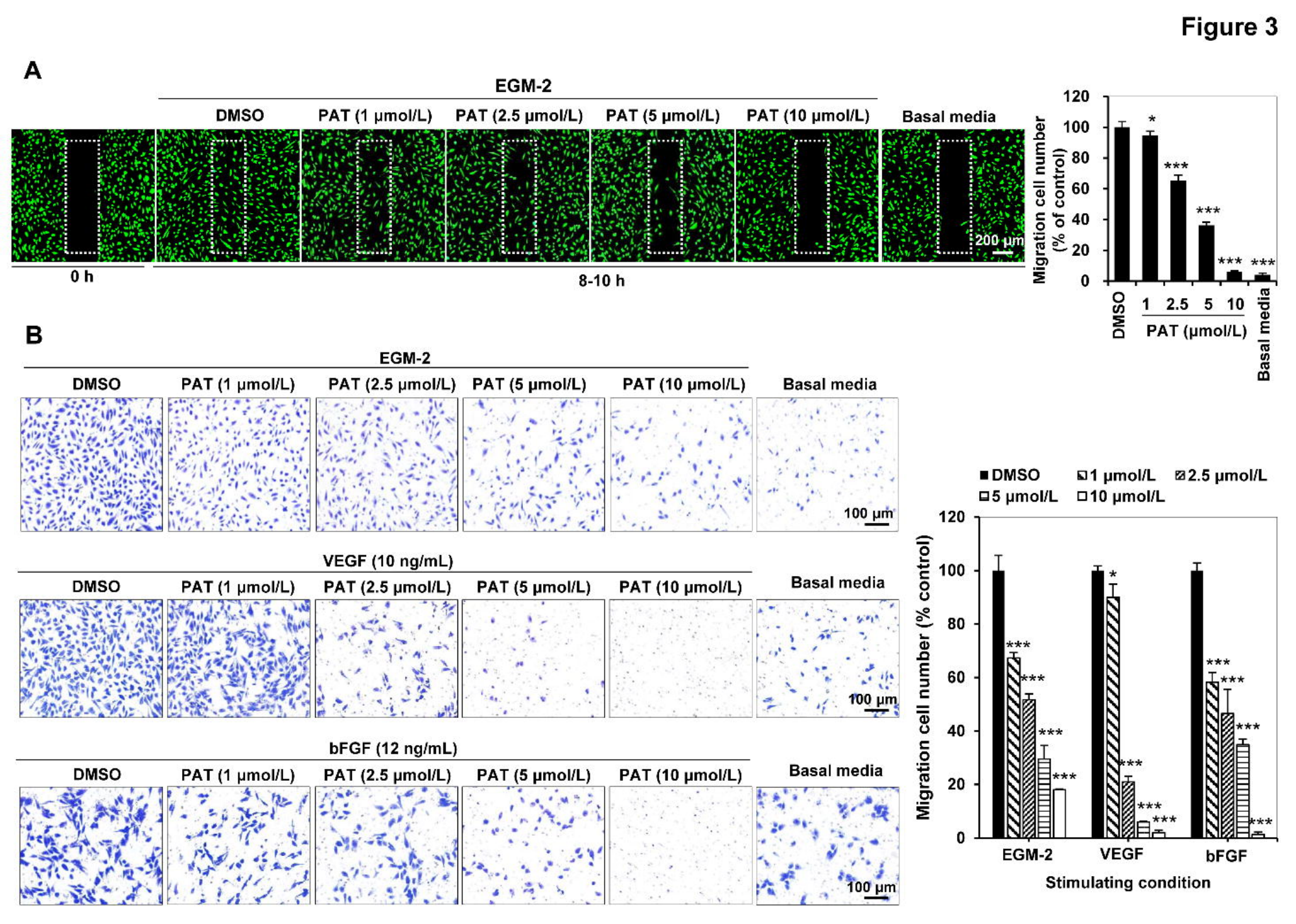
A
EGM-2
DMSO
PAT (1 μmol/L)
PAT (2.5 μmol/L)
PAT (5 μmol/L)
PAT (10 μmol/L)
Basal media
200 μm
0 h
8-10 h
Migration cell number (% of control)
120
100
80
60
40
20
0
*
***
***
***
***
DMSO
1
2.5
5
10
PAT (μmol/L)
Basal media
B
EGM-2
DMSO
PAT (1 μmol/L)
PAT (2.5 μmol/L)
PAT (5 μmol/L)
PAT (10 μmol/L)
Basal media
100 μm
VEGF (10 ng/mL)
bFGF (12 ng/mL)
DMSO
1 μmol/L
2.5 μmol/L
5 μmol/L
10 μmol/L
Migration cell number (% control)
EGM-2
VEGF
bFGF
Stimulating condition

Figure 4

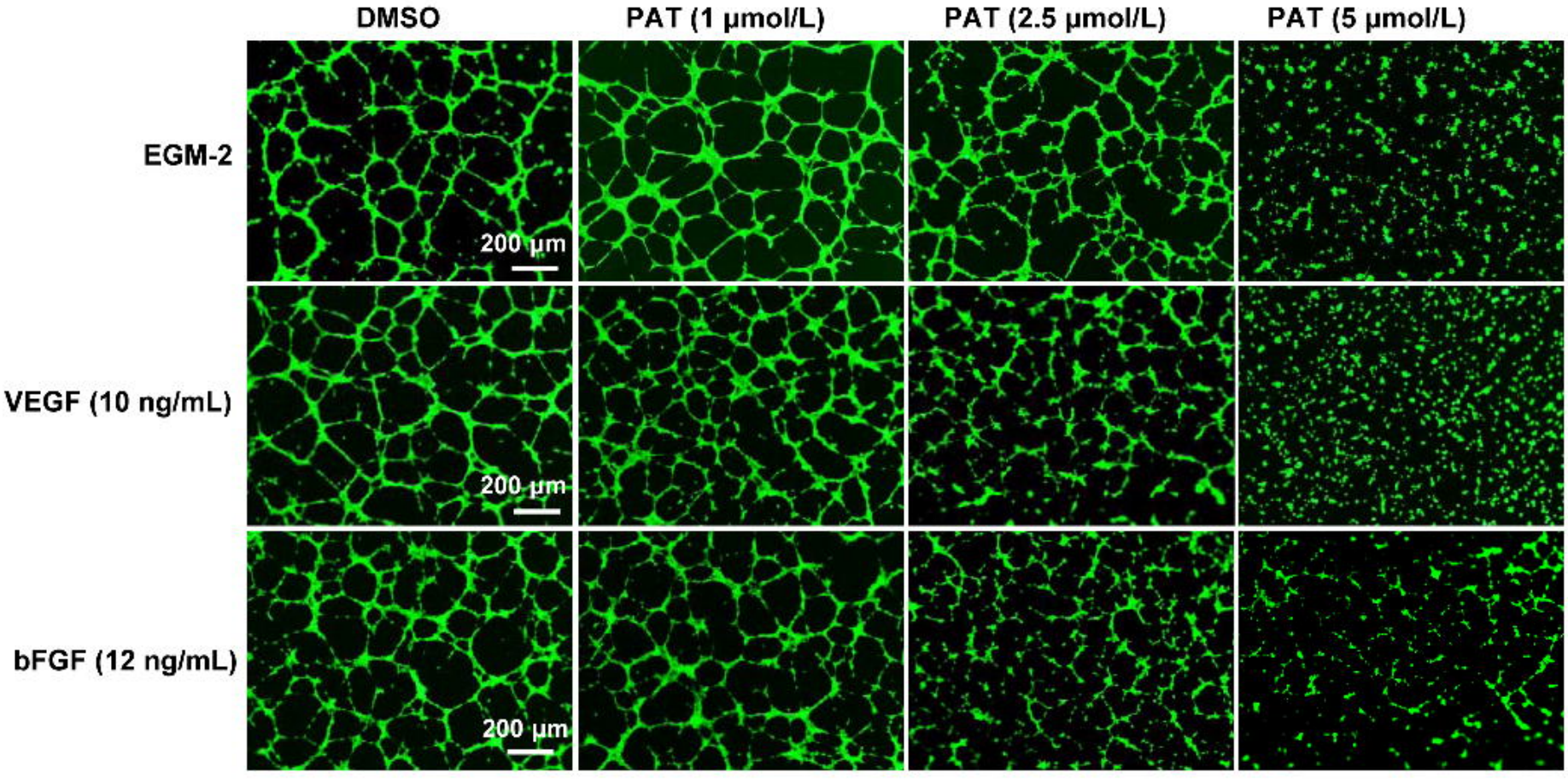
DMSO
PAT (1 μmol/L)
PAT (2.5 μmol/L)
PAT (5 μmol/L)
EGM-2
VEGF (10 ng/mL)
bFGF (12 ng/mL)
200 μm
200 μm
200 μm

Figure 5

A


Control
VEGF
VEGF+PAT (10 μmol/L)
VEGF+PAT (50 μmol/L)

B

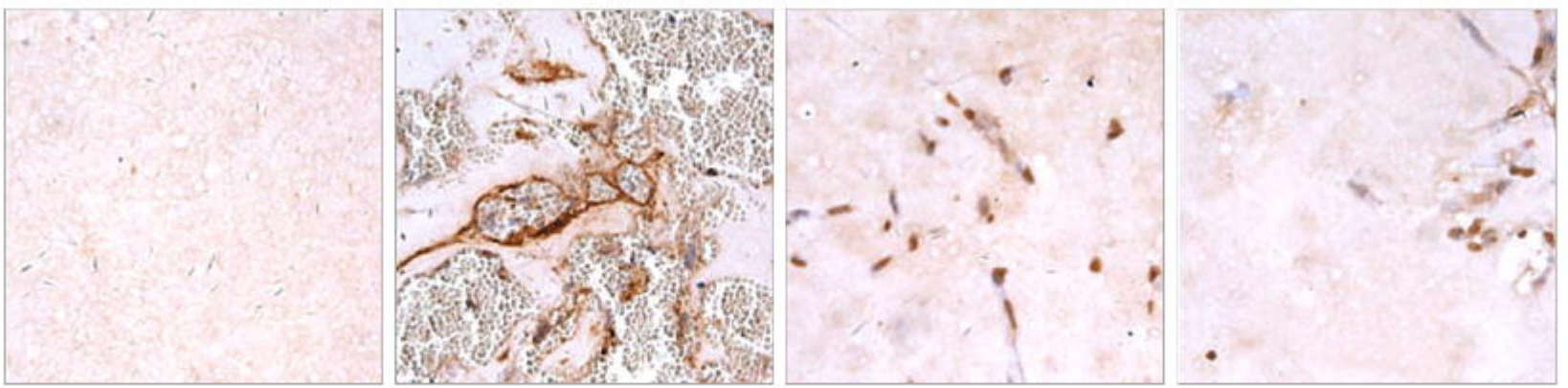
Control
VEGF
VEGF+PAT (10 μmol/L)
VEGF+PAT (50 μmol/L)

Figure 6

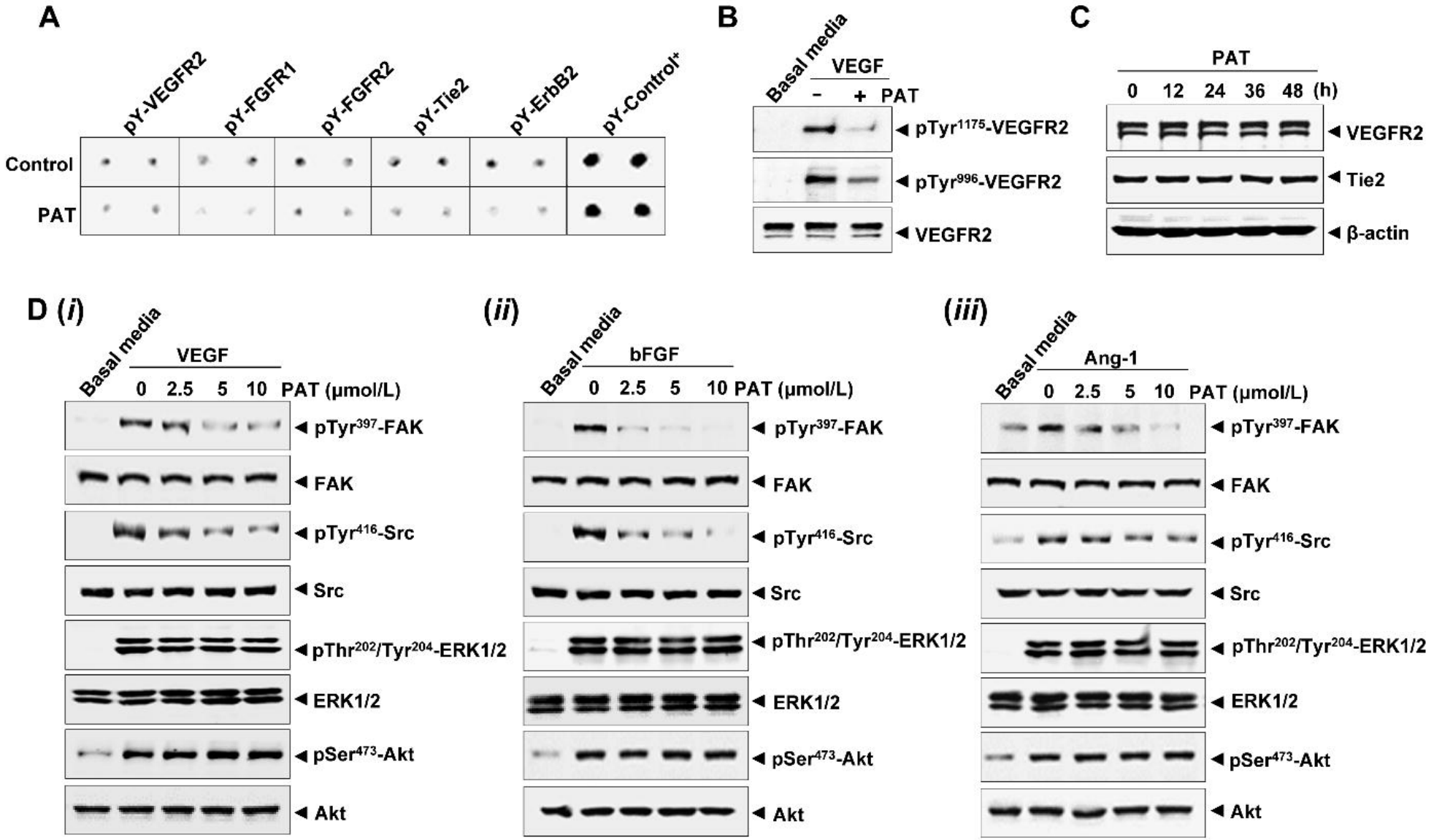
A
pY-VEGFR2
pY-FGFR1
pY-FGFR2
pY-Tie2
pY-ErbB2
pY-Control*
Control
PAT
B
Basal media
VEGF
- + PAT
pTyr1175-VEGFR2
pTyr996-VEGFR2
VEGFR2
C
PAT
0 12 24 36 48 (h)
VEGFR2
Tie2
β-actin
D (i)
Basal media
VEGF
0 2.5 5 10 PAT (μmol/L)
pTyr397-FAK
FAK
pTyr416-Src
Src
pThr202/Tyr204-ERK1/2
ERK1/2
pSer473-Akt
Akt
(ii)
Basal media
bFGF
0 2.5 5 10 PAT (μmol/L)
pTyr397-FAK
FAK
pTyr416-Src
Src
pThr202/Tyr204-ERK1/2
ERK1/2
pSer473-Akt
Akt
(iii)
Basal media
Ang-1
0 2.5 5 10 PAT (μmol/L)
pTyr397-FAK
FAK
pTyr416-Src
Src
pThr202/Tyr204-ERK1/2
ERK1/2
pSer473-Akt
Akt